Design Concepts for Controlled Rocking of Self-Centering Steel-Braced Frames

Matthew R. Eatherton, M.ASCE[1]; Xiang Ma, A.M.ASCE[2]; Helmut Krawinkler, M.ASCE[3]; David Mar[4]; Sarah Billington, M.ASCE[5]; Jerome F. Hajjar, F.ASCE[6]; and Gregory G. Deierlein, F.ASCE[7]

Abstract: The self-centering rocking steel-braced frame is a high-performance system that can prevent major structural damage and minimize residual drifts during large earthquakes. It consists of braced steel frames that are designed to remain elastic and allowed to rock off their foundation. Overturning resistance is provided by elastic post-tensioning, which provides a reliable self-centering restoring force, and replaceable structural fuses that dissipate energy. The design concepts of this system are examined and contrasted with other conventional and self-centering seismic force resisting systems. Equations to predict the load-deformation behavior of the rocking system are developed. Key limit states are investigated including desired sequence of limit states and methods to help ensure reliable performance. Generalized design methods for controlling the limit states are developed. The design concepts are then applied to a six-story prototype structure to illustrate application of the rocking steel frame system and provide the framework for a coordinated research program to further develop and validate the concepts. **DOI: 10.1061/(ASCE)ST.1943-541X.0001047.**

Author keywords: Self-centering; Structural fuses; Large-scale experiments; Seismic force resisting system; Earthquake repairability; Controlled rocking; Spine systems; Seismic effects.

Introduction

Conventional seismic force-resisting systems rely on inelastic deformations in primary structural members to dissipate seismic energy and protect buildings against collapse. While current building code requirements are generally considered to provide adequate safety, their prescriptive requirements that focus on lateral strength and ductility do not explicitly control the amount of structural and nonstructural damage or provide for continued use after the earthquake. The resulting earthquake damage to primary structural members, including braces, walls, beams, columns, and connections, and residual drifts can result in buildings that are difficult and financially prohibitive to repair after a large earthquake.

Performance-based earthquake engineering highlights the importance of reducing repair costs and avoiding building closures, which can otherwise result in business interruption and displacement of occupants. Higher performance can be achieved by minimizing inelastic deformation and damage to primary structural components and residual drifts. In general, it is neither practical nor economical to strengthen conventional seismic systems to achieve this performance. Instead, new approaches are needed, such as the rocking frames described herein where inelastic deformations are concentrated in replaceable ductile fuses, and where self-centering systems maintain building plumb and practically eliminate residual drifts.

The proposed self-centering rocking braced frame has a stiff vertical spine with an articulated rocking mechanism, designed so that the spine remains essentially elastic outside of designated replaceable energy-dissipating elements. The system is capable of preventing major structural damage and residual drift when subjected to severe maximum considered earthquake (MCE) level ground motion intensities. Fig. 1 shows one possible configuration of the rocking frame; other configurations with alternative post-tensioning and fuse locations are discussed later. The system consists of three main components:

1. A steel braced frame that remains essentially elastic by uplifting at the column bases during ground motions. The rocking frame creates a stiff spine that promotes uniform story drifts up the building, and the column base detail permits uplift while restraining horizontal motion through bearing against bumper supports;
2. Vertical post-tensioning (PT) that provides resistance to overturning and provides self-centering forces. The initial stress in the strands is selected so as to provide sufficient uplift resistance while allowing for sufficient straining capacity to remain elastic under expected rocking; and
3. Replaceable energy-dissipating elements that resist overturning and act as structural fuses that yield, effectively limiting the forces imposed on the rest of the structure.

[1]Assistant Professor, Dept. of Civil and Environmental Engineering, 105D Patton Hall, Virginia Tech, Blacksburg, VA 24061 (corresponding author). E-mail: meather@vt.edu

[2]Consultant, McKinsey & Company, Chicago, IL 60603. E-mail: maxiangnu@gmail.com

[3]Professor, Dept. of Civil and Environmental Engineering, Y2E2 Building Room 231, Stanford Univ., Stanford, CA 94305. E-mail: krawinkler@stanford.edu

[4]Principal, Tipping Mar, 1906 Shattuck Ave., Berkeley, CA 94704. E-mail: david.mar@tippingmar.com

[5]Professor, Dept. of Civil and Environmental Engineering, 473 Via Ortega, Room 285A, Stanford Univ., Stanford, CA 94305. E-mail: billington@stanford.edu

[6]Professor and Chair, Dept. of Civil and Environmental Engineering, 400 Snell Engineering Center, 360 Huntington Ave., Northeastern Univ., Boston, MA 02115. E-mail: jf.hajjar@neu.edu

[7]Professor, Dept. of Civil and Environmental Engineering, Blume Earthquake Engineering Center Room 118, Stanford Univ., Stanford, CA 94305. E-mail: ggd@stanford.edu

Note. This manuscript was submitted on May 22, 2013; approved on February 6, 2014; published online on May 21, 2014. Discussion period open until October 21, 2014; separate discussions must be submitted for individual papers. This paper is part of the ***Journal of Structural Engineering***, © ASCE, ISSN 0733-9445/04014082(11)/$25.00.

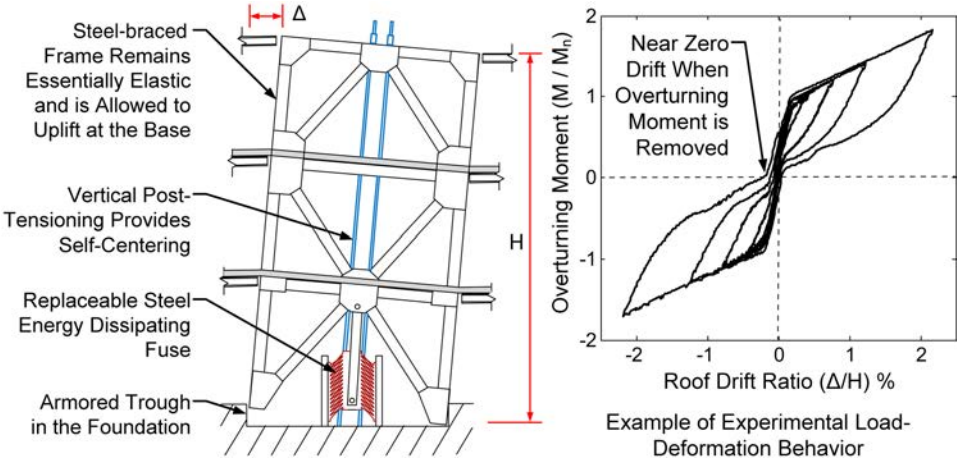

Fig. 1. Description of the controlled rocking system

The self-centering rocking braced frame has been developed and investigated through a multi-institution, international research project. Components of the research are illustrated in Fig. 2 and include three experimental programs with complementary computational studies. The fuse elements were developed, analyzed, and tested at Stanford University (Ma et al. 2010). Half-scale quasi-static cyclic and hybrid simulation tests were conducted at the University of Illinois at Urbana Champaign to investigate system and component behavior and refine construction details (Eatherton and Hajjar 2010; Eatherton et al. 2014). Shake table tests of a two-thirds scaled specimen were conducted at the E-Defense facility in Japan to validate system performance and investigate dynamic system behavior (Ma et al. 2011). Computational studies were conducted to investigate (1) the effect of system parameters (Hall et al. 2010), (2) the required restoring force to reliably self-center a complete building system (Eatherton and Hajjar 2011), and (3) the overall design and performance of controlled rocking systems (Eatherton and Hajjar 2010; Ma et al. 2011).

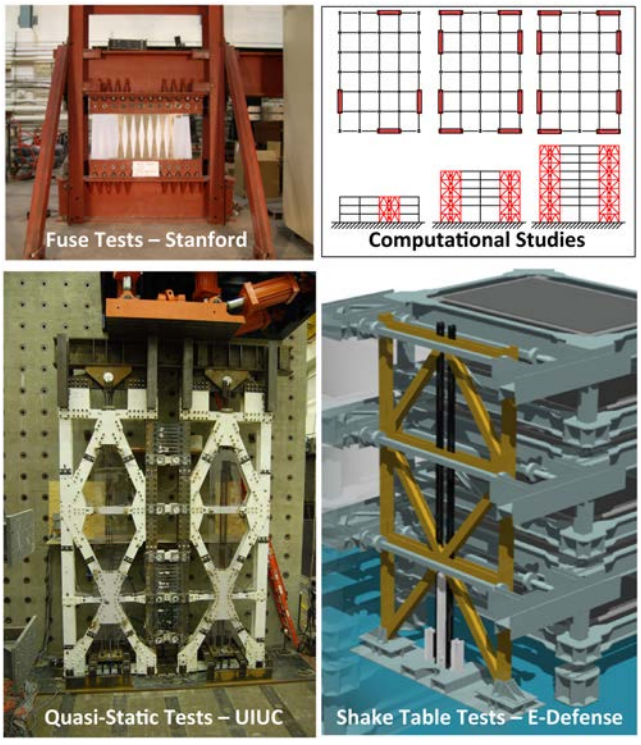

Fig. 2. Graphical depiction of project phases

This paper draws from all phases of this project to describe the key design concepts for self-centering rocking steel frames. First, previous work on seismic force-resisting systems that incorporate self-centering capability and structural fuses are examined. Alternative rocking frame configurations are then discussed followed by the development of key equations and considerations for their seismic design. Finally, the concepts are illustrated through a design example.

Impact of Residual Drifts on Building Performance

Residual drifts are often a determining factor in whether a structure can be repaired or occupied after an earthquake, which in turn contributes to the economic losses related to repair or replacement costs and business downtime. In a study of buildings damaged in the 1995 Hyogoken-Nanbu earthquake, structures with residual drift ratios greater than 0.5% had issues with egress following the earthquake and were expensive to repair (McCormick et al. 2008), and buildings with roof drift ratios greater than 1% and story drift ratios greater than 1.4% were demolished (Iwata et al. 2006). The expected residual drifts in buckling restrained braced frame buildings were analyzed based on several model buildings resulting in a median residual story drift ratio of 0.5% for design basis earthquake (DBE) ground motions and 1.2% for MCE ground motions (Fahnestock et al. 2007). Similar median residual interstory drift ratios were reported for concentrically braced frames: 0.6% and 1.6% for DBE and MCE levels, respectively (Lai et al. 2010). The recently published FEMA P-58 (ATC 2012) *Seismic Performance Assessment of Buildings* incorporates provisions to incorporate the risk of demolition associated with residual drifts in the loss assessment and in a recent study to evaluate the performance of a modern code-conforming concrete building, Ramirez and Miranda (2012) show that residual drifts can significantly contribute to the overall earthquake loss.

Residual drifts also impact whether buildings are safe for occupancy after an earthquake. Studies by Bazzurro et al. (2004) and Luco et al. (2004) identify residual drifts as an important factor affecting the safety of buildings to resist aftershocks, and the ATC 20 guidelines for post-earthquake inspections of buildings (ATC 1995)

identify those with noticeable out of plumb to be considered as unsafe with restricted access. These are just a few of the studies that illustrate the significant impact that residual drifts can have on the economic losses and post-earthquake function of buildings. With the potential to practically eliminate residual drifts, the rocking frame systems can dramatically reduce building losses and, thereby, improve community resilience.

Background on Rocking Systems

Previously, researchers have studied rocking of stone monuments, building foundations on soil, masonry wall piers, concrete walls, bridge piers, and steel-braced frames. Through many of the studies, it has been shown that structures undergoing rocking motion produce lower seismic base shear with reduced ductility demands on the structural elements than their fixed-base counterparts. The effect of radiation damping, a form of energy dissipation that occurs as the uplifting side contacts the base, has been studied and converted to an equivalent viscous damping ratio of 2 to 6% for some typical configurations (e.g., Housner 1963; Mander and Cheng 1997; Ajrab et al. 2004). Vertical accelerations and forces due to vertical modes excited by the impact have also been studied (e.g., Pollino and Bruneau 2004; Chen et al. 2006) and in some cases found to approximately double the vertical forces in a set of example rocking steel bridge piers (Pollino and Bruneau 2004). Lu (2005) identified a three-dimensional effect that occurs when an uplifting column or edge of a wall is attached to surrounding floor framing, and a restoring force is created as the floor framing resists the upward movement.

Rocking of steel structures has been investigated in several studies. Clough and Huckleridge (1977) performed some of the earliest shaking table tests on rocking steel frames, which demonstrated the potential benefits of rocking. Researchers in Japan have shown that yielding base plates, which allow some uplift while dissipating energy, can reduce the seismic response of moment frames and braced frames (Azuhata et al. 2006), and researchers in Canada have explored using hydraulic dampers at the column bases to reduce seismic response (Tremblay et al. 2008). Other researchers have studied multiple uplifting locations up the height of braced frames (Weibe and Christopoulos 2009), including implementations of this concept in industrial storage buildings (Wada et al. 2001). Hybrid simulation experiments have been conducted on large-scale rocking steel-braced frames, similar to those examined in this paper (Sause et al. 2010), and the forces developed in rocking braced frames have been investigated (Roke et al. 2009; Pollino and Bruneau 2004). Rocking braced steel frames have also been incorporated into actual buildings, including the Victoria University of Wellington Student Accommodation Building (Gledhill et al. 2008), the Orinda City Hall (Mar 2010), the Packard Foundation Headquarters in California (Tipping-Mar 2012), and the Hollywood Casino in Missouri (GLPA 2012).

Rocking mechanisms have been incorporated into masonry and concrete structures (e.g., Priestley et al. 1999). Seismic design provisions for precast systems have been developed and adopted for design by reference as providing behavior that is at least equivalent to cast-in-place shear walls (ACI ITG 2009).

The present study builds upon these examples of previous research on rocking behavior and applications to seismic design to further develop and validate design concepts and criteria for a specific type of rocking steel-braced frames.

Rocking Steel Frame Configurations and Implementation

The main three components of the proposed self-centering rocking frame system, i.e., the rocking frame, the PT, and the energy-dissipating fuse, can be arranged in different configurations. The single-frame system, shown in Fig. 1, is repeated in Fig. 3(a) to contrast it with the dual-frame configuration shown in Fig. 3(b). The single-frame configuration [Fig. 3(a)] utilizes two shear fuse elements that are anchored on their edges with their center connected to the frame that displaces upward during rocking. The dual frame configuration [Fig. 3(b)] has shear yielding elements between two rocking frames. Alternate fuse elements, such as buckling restrained braces (BRB), have also been investigated [Fig. 3(c)], and other configurations are possible, including those with fuse elements attached to the base of the columns and vertical PT located at the column lines [Fig. 3(d)]. These are just an illustration as to the variety of possible configurations of frames, PT, and fuses.

As illustrated in Fig. 4, the rocking steel frames can be implemented as the seismic resisting system in place of a conventional

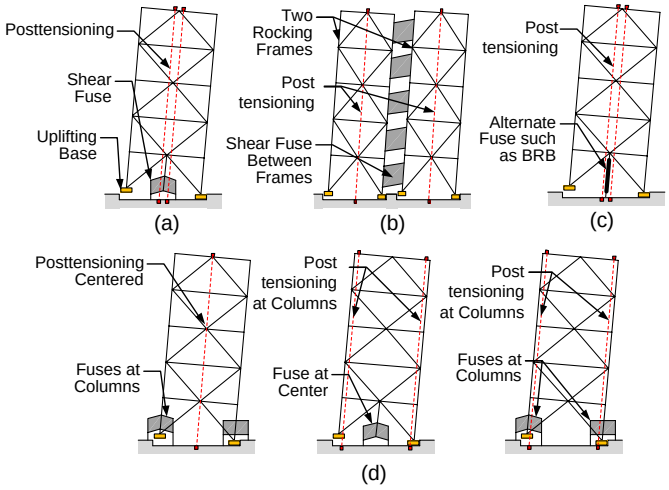

Fig. 3. Potential system configurations including (a) single-frame configuration; (b) dual-frame configuration; (c) alternate fuse type; (d) alternate locations for components

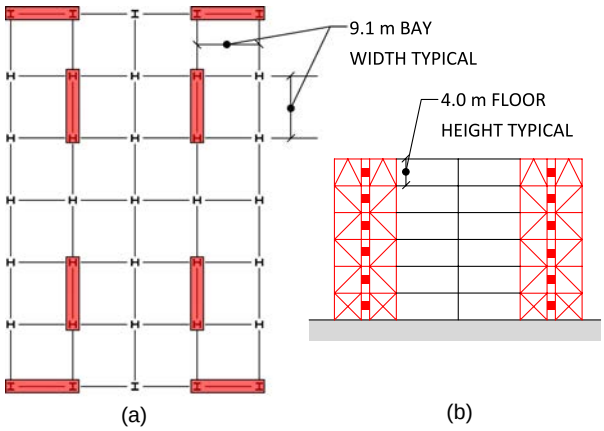

Fig. 4. Typical structural framing for rocking frame seismic system: (a) prototype building plan; (b) prototype building evaluation

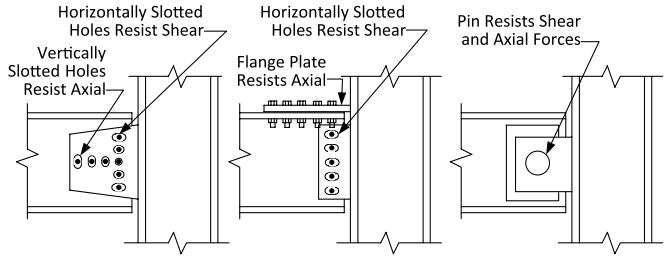

Fig. 5. Collector beam details to uplifting rocking frame columns

braced frame at interior or exterior framing bays. When the rocking frame is connected to the diaphragm using conventional floor framing construction, the rocking action will lift the floor systems, which may result in some localized floor slab damage in the vicinity of the uplifting columns after large earthquakes. The uplift that develops in the floor system during rocking can be estimated assuming rigid body rotation of the frames and linear deflection of the floor beams. A modified collector detail in the bays directly adjacent to the rocking frame may be necessary to accommodate the rotation associated with the uplifting column. Examples of collector connection details, shown in Fig. 5, include details with slotted holes or a pin to allow rotation. Alternative framing details for isolating the floor from vertical motion of the rocking frame, and thereby avoiding any floor slab damage, have been proposed in Eatherton and Hajjar (2010). Where the rocking frames are located along the building perimeter, consideration should be given to detailing the building façade to accommodate the vertical rocking deformations.

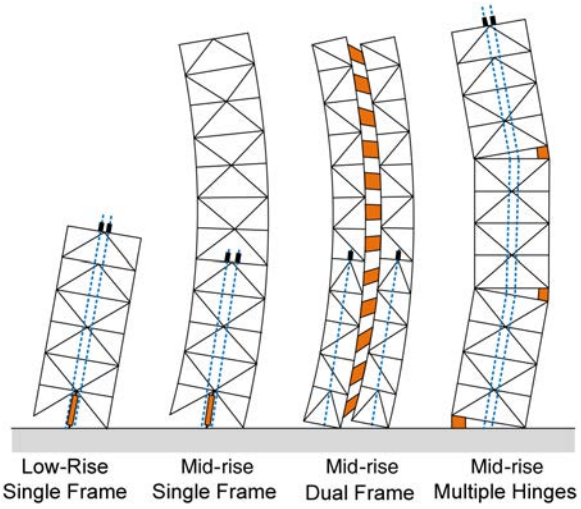

Fig. 6. Rocking frame behavior at different heights

Variations in system behavior as the height of the structure increases are demonstrated in Fig. 6. For low-rise rocking systems, the frame is intended to remain essentially elastic leading to a stiff spine that enforces a near-linear mode shape. As the building height and frame slenderness increases, flexural deformation and higher mode effects will become more significant. The first mode response of the elastic spine systems is generally controlled by the base overturning response, which is associated with the rocking resistance that is related to design of the post-tensioning and fuses. Thus the proposed design procedures for the post-tensioning and fuses are primarily related to the first-mode behavior, which is the dominant mode of inelastic response for low-rise and midrise structures. The steel-braced frames, on the other hand, are intended to elastically resist the forces associated with all vibration modes and must be designed to resist forces associated with the inelastic first-mode demands and elastic higher mode demands. The behavior of single frame configurations applied to midrise buildings is similar to concrete shear walls that are designed to remain essentially elastic outside of the flexural hinge region at the base. When implemented in the dual frame configuration, the midrise rocking frame behaves like a coupled concrete shear wall with flexural hinges at the base of each wall. A variation on this behavior, shown on the right of Fig. 6, includes multiple flexural hinges along the height of the structure, which has been shown to reduce the elastic shear and moment demands on the intermediate floors (Wiebe and Christopoulos 2009).

The butterfly steel fuses, developed in this research, are shown in Fig. 7. The active portion of the fuse is a mild steel plate with diamond-shaped holes fabricated using laser or water jet cutting. The resulting steel links have a butterfly shape that is optimized to distribute yielding and provide high ductility. In the single-frame configuration, butterfly links are located on each side of a strut that is connected to the rocking frame [Fig. 7(a)]. As the frame rocks, the strut and center of the fuse plates are pulled upward and pushed downward, cyclically yielding the butterfly links to resist overturning and dissipate energy. In the dual-frame configuration [Fig. 7(b)] the butterfly fuse plates are connected between the interior columns of the two rocking frames, acting as shear links that are cyclically yielded.

Development of the butterfly fuse plates including testing is described in Ma et al. (2010) and the behavior of the fuses in the rocking steel frame system are described in Ma et al. (2011)

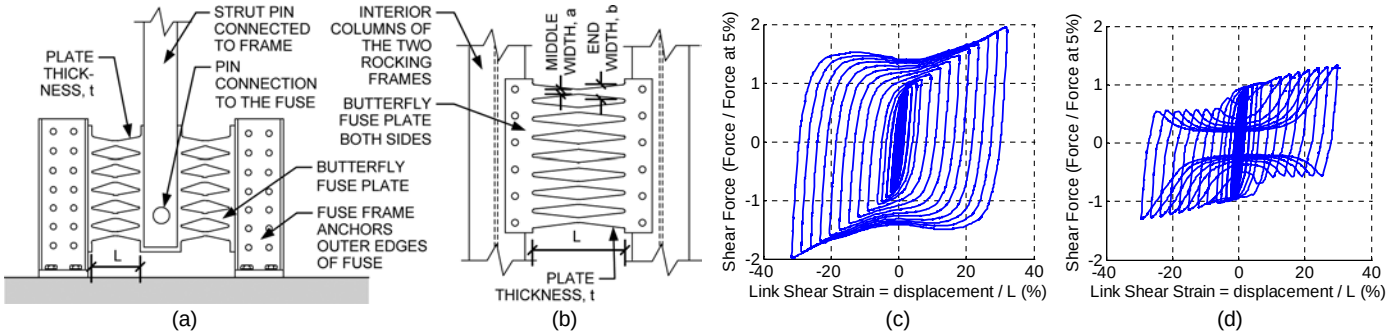

Fig. 7. Examples of butterfly shear fuse plates configurations and types of behavior: (a) single-frame configuration; (b) dual-frame configuration; (c) nondegrading behavior; (d) degrading behavior

and Eatherton and Hajjar (2010). These tests demonstrated that hysteretic behavior of the butterfly plates can be altered by adjusting the plate dimensions. For example, Figs. 7(c and d) contrast the hysteretic behavior of fuse plates with differing slenderness. The two fuse plates have the same geometry (link length, L = 356 mm, and link end width, b = 19 mm), except that one has a thicknesses of 25 mm versus 6 mm in the second case. At link shear deformations of about 10%, the links of the thin fuse plate experience lateral torsional buckling, leading to a pinched hysteretic response [Fig. 7(d)] and a reduction in energy dissipation. The resulting strength degradation reduces the resistance to self-centering, which when properly balanced can improve the overall self-centering performance of the rocking frame system. This behavior is in contrast to large-strain hardening that occurs in the hysteretic response of the thicker fuse [Fig. 7(c)].

Rocking Steel Frame Behavior

The behavior of the controlled rocking system for steel braced frames can be characterized by the actions of the PT frame and fuse components. Fig. 8(a) shows the idealized nonlinear elastic load-deformation behavior of the PT braced frame system. The elastic frame stiffness, K_{fr}, controls the response before the frame experiences uplift at a moment, M_{up}. As the frame uplifts, the PT strands elongate elastically, creating the post-uplift stiffness, K_{up}. The fuse system, shown in Fig. 8(b), is assumed to exhibit elastic–linear hardening hysteretic response similar to the nondegrading fuse behavior shown in Fig. 7(c), where the yield strength, M_{fsy}, and pre-uplift and post-uplift stiffness, K_{fs} and K_{fh}, are calculated based on the fuse geometry and materials (details provided in Ma et al. 2010).

When these two components are combined in parallel, the resulting load-deformation response is shown in Fig. 8(c) and found to generally agree with observed behavior (e.g., see Fig. 1). The flag-shaped hysteretic behavior is characteristic of the self-centering system where the lateral drift returns to near zero as the force is removed. The combined hysteretic response can be characterized by three stiffnesses, K_1, K_2, and K_3, a system yield moment, M_y, and a flag height, M_{flag}. The initial stiffness, K_1, is the sum of the elastic frame stiffness, K_{fr}, and the initial fuse stiffness, K_{fs}. With a few notable exceptions (e.g., the midrise dual frame shown in Fig. 6), the fuse stiffness will be small compared to the frame stiffness. The second and third stiffnesses, K_2 and K_3, are the sum of the frame uplifting stiffness, K_{up}, plus the initial fuse stiffness, K_{fs}, and the sum of the uplifting stiffness, K_{up}, plus the fuse hardening stiffness, K_{fh}, respectively. After the initial uplift cycle, the K_1 and K_2 stiffness branches revert to a single branch with a reduced stiffness, due to the presence of residual forces that develop in the yielded fuse, as represented by the dashed lines in Figs. 8(b and c).

The yield moment, M_y, is given by Eq. (1), which can be simplified as shown to neglect the terms associated with additional elongation of the PT strands between uplift and fuse yield, if the uplifting stiffness, K_{up}, is small relative to the frame stiffness, K_{fr}, and the elastic fuse stiffness, K_{fs}. The uplifting moment and fuse yield moment are given by Eqs. (2) and (3) as functions of the initial PT force, F_{pti}, the expected dead loads acting on the rocking frame, P_{De}, the fuse yield force, V_{fp} and their respective eccentricities, X_{PT}, X_D, and X_{fs}, relative to the rocking pivot point. Refer to Fig. 9 for the associated dimensions for the single-frame and dual-frame configurations. Assuming rigid body rotation of the frame, the post-uplift stiffness K_{up} can be calculated using Eq. (4) as a function of the effective elastic modulus of the PT, E_{pt}, the area of the PT, A_{pt}, eccentricity of the PT relative to the pivot point, X_{PT}, number of frames, N_{frames} (1 for single, 2 for dual), and length of the PT, L_{pt}. The moment associated with an arbitrary drift ratio, δ/H, after the fuse has yielded is given in Eq. (5), and the height of the hysteretic flag shape is given in Eq. (6)

$$M_y = M_{\text{up}}\left(1 - \frac{K_{\text{up}}}{K_{fr}}\right) + M_{\text{fsy}}\left(1 + \frac{K_{\text{up}}}{K_{fs}}\right) \cong M_{\text{up}} + M_{\text{fsy}} \quad (1)$$

$$M_{\text{up}} = \sum F_{\text{pti}} X_{\text{PT}} + \sum P_{De} X_D \quad (2)$$

$$M_{\text{fsy}} = \sum V_{fp} X_{fs} \quad (3)$$

$$K_{\text{up}} = \frac{X_{PT}^2}{L_{pt}} E_{pt} A_{pt} N_{\text{frames}} \quad (4)$$

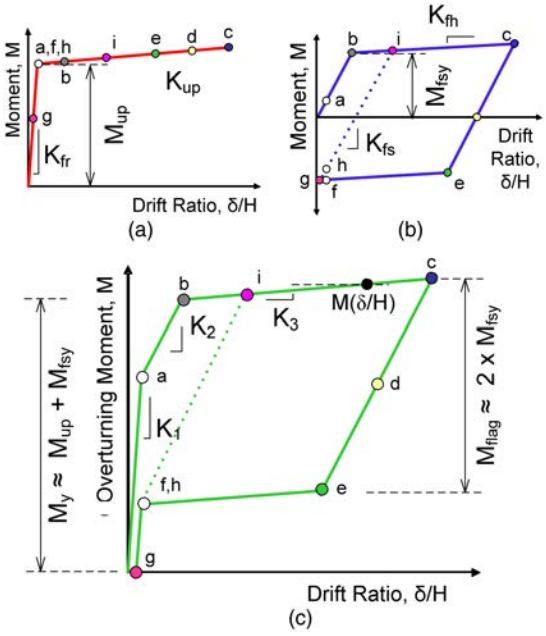

Fig. 8. Force-deformation behavior of the (a) post-tensioned frame; (b) system with fuses only; (c) combined system response

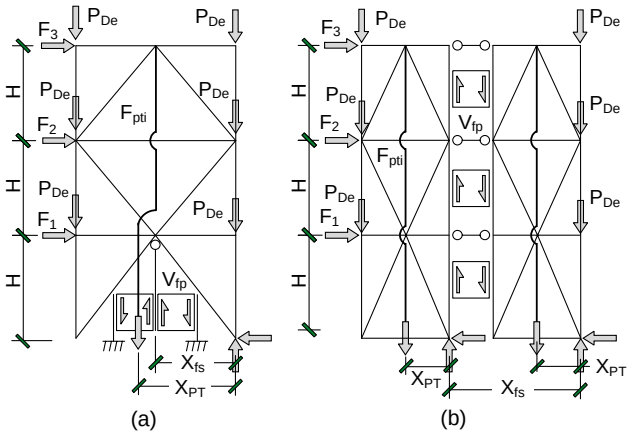

Fig. 9. Frame geometry and variable definitions: (a) single frame; (b) dual frame

$$M\left(\frac{\delta}{H}\right) = M_y + \left(\frac{\delta}{H}\right)(K_{\text{up}} - K_{fh}) \tag{5}$$

$$M_{\text{flag}} = 2M_{\text{fsy}}\left(1 + \frac{K_{\text{up}}}{K_{fs}}\right) \cong 2M_{\text{fsy}} \tag{6}$$

Limit States

Reliable seismic behavior of the controlled rocking braced steel-frame system depends on understanding and controlling the sequence of limit states. Consider the cyclic response shown in Fig. 10, where the key limit states include (1) initial uplift, (2) fuse yielding, (3) onset of yielding in PT that leads to (4) loss of full self-centering capability, and finally (5) overall strength degradation, which can result from fuse fracture, PT fracture, or frame failure. The behavior shown in Fig. 10 assumes that global uplift (an undesirable limit state in which the PT force is insufficient to force fuse yielding that is discussed further below) is prevented and the definition of full self-centering is based on the lateral resistance of the rocking frame by itself neglecting the resistance of the building's gravity framing. Methods for controlling these limit states are discussed below, based on Eqs. (1)–(3) and (6), and considering the following design parameters (shown in Fig. 9): initial PT force, F_{pti}, a total fuse shear yield force, V_{fp}, eccentricities, X_{fs}, X_{PT}, and X_D described above, and floor heights, H_1, H_2, and H_3. The applied loads include lateral earthquake forces, F_1, F_2, and F_3, which for the sake of this discussion could be calculated using the equivalent lateral force method of ASCE 7 (ASCE 2010).

The primary design parameter is the system overturning strength, which can be assessed using the limit state equation given in Eq. (7). Assuming that the response is dominated by first-mode behavior, the required overturning moment, M_u, is given by Eq. (8) where F_i is the lateral load determined by an equivalent lateral force procedure and H_i is the height of the lateral load above the rocking interface. To provide comparable yield strengths to other ductile seismic systems, the lateral design forces, F_i, can be determined using a minimum base shear with an assumed seismic response factor, R, as is done for other systems in ASCE 7. A value of R equal to 8 is proposed to achieve comparable yield strengths as other ductile seismic systems. Tests and analyses conducted as part of this research, including a limited FEMA P695 (FEMA 2009) study to assess collapse safety (Ma et al. 2011), further confirm that systems designed with R equal to 8 can readily satisfy other critical safety limit states required as part of the proposed design method. The nominal overturning resistance, M_n, is then assumed to be equal to the yield moment, M_y, [Eq. (1)], where the terms are as defined previously. For consistency with standard load and resistance factor formulations, a resistance factor, ϕ, is applied in calculating the design resistance

$$M_u \le \phi M_n \quad [\text{where } M_n = M_y, \text{per Eq. (1)}] \tag{7}$$

$$M_u = \sum_{i=1}^{\text{Floors}} F_i H_i \tag{8}$$

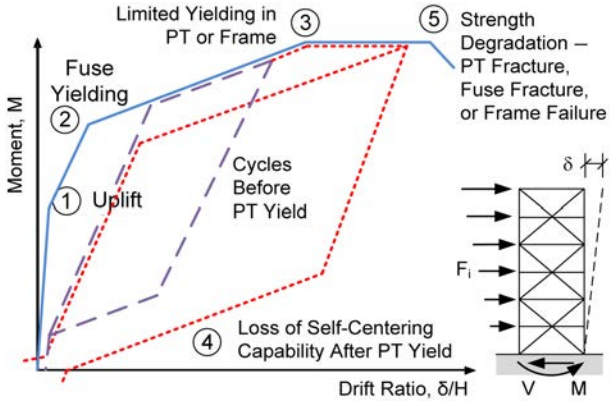

Fig. 10. Rocking behavior and limit states

Self-Centering

The self-centering limit state, implying the system will return to near zero drift when the inertial lateral loads are removed, is controlled by the relative magnitudes of the self-centering restoring forces to the resisting forces. As described by Eq. (9), the self-centering ratio, SC, is defined as the ratio of restoring moment, M_{up}, provided by the initial PT force and dead load [Eq. (2)], to the resisting moment, M_{fsy}, defined by the yield strength of the energy dissipating elements [Eq. (3)]

$$\text{SC} = \frac{M_{\text{up}}}{M_{\text{fsy}}} \tag{9}$$

$$F_{\text{pti}}* = A_{\text{PT}}[\sigma_{pti} - (\varepsilon_{\text{peak}} E_{\text{PT}} - \sigma_{\text{PTy}})] \tag{10}$$

It should be emphasized that the SC ratio, given by Eq. (9), is a convenient index of the tendency to self-center, but it does not fully describe the entire range of behavior that may occur during loading and unloading. For example, to completely describe the self-centering characteristic at the peak point in a loading excursion, the restoring moment would need to be modified to account for increase in PT force due to elastic straining [considering K_{up} in Eqs. (4) and (5) and the resisting moment would be adjusted to account for inelastic strain hardening (or softening) of the energy dissipating fuse (Fig. 7). In the unloaded condition, the restoring and resisting moments would similarly need to be modified to account for PT losses, due to yielding and seating of the PT (e.g., yielding beyond point 3 in Fig. 10), and the residual resistance of the yielded fuse. The PT force after losses due to yielding, $F_{\text{pti}}*$, can be calculated using Eq. (10) as a function of the initial PT stress, σ_{PTi}, the peak PT strain, $\varepsilon_{\text{peak}}$, as calculated below in Eq. (13), and the yield stress of the PT, σ_{PTy}. PT losses due to seating can be minimized by power-seating the PT wedge anchors or seating the wedges under high stresses (e.g., $0.9\sigma_{Pty}$) and then backing the stress down to the desired initial PT (e.g., by installing and removing shims beneath the PT anchorage). The seating losses can be calculated by multiplying the estimated seating displacement (typically a few millimeters) by the tendon stiffness $A_{\text{PT}}E_{\text{PT}}/L_{\text{PT}}$. The fuse yield strength after hardening, $V_{fp}*$, may be determined based on the fuse-hardening slope, K_{fh}, (determined from tests) and a specified drift demand. In addition to changes in the PT and fuse forces, the simple SC index does not account for the lateral force resistance of the gravity framing system and other components of the building (e.g, architectural partitions) that may inhibit self-centering. These additional effects were investigated by Eatherton and Hajjar (2011) for representative steel-framed office buildings and found not to significantly impair the ability of the lateral rocking system to self-center the entire building when the effective SC ratio is larger than unity.

Global Uplift

Another limit state check that is associated with the ratio of force in the PT versus energy-dissipating fuses is the undesirable condition where the braced frame undergoes global uplift rather than rocking on its base. Global uplift occurs when the upward fuse yield strength acting on the frame is greater than the downward forces provided by the PT and expected dead load. The global uplift can be evaluated using the uplift ratio, UL, of Eq. (11), where uplift is prevented when the ratio is greater than unity. Note that for dual frame configurations, Eq. (11) should be calculated separately for each frame, based on the forces acting on the frame. For single-frame configurations where the rocking pivot arms are the same for the PT, dead load, and fuse, the UL and SC ratios are equivalent. As discussed above with regard to self-centering, it may be appropriate to consider PT force after losses, F^*_{PT}, and hardened fuse capacity, V^*_{fp}, associated with a specified peak displacement (e.g., design basis earthquake drifts) in this calculation

$$\mathrm{UL} = \frac{\sum F_{\mathrm{pti}} + \sum P_{De}}{\sum V_{fp}} \geq 1.0 \tag{11}$$

Minimum Energy Dissipation

Controlling the potential for strength degradation limit states (shown as Point 5 on Fig. 10) requires consideration of the expected peak drifts during an earthquake and the ability of the system to resist strength-degrading events, such as significant PT fracture, fuse fracture, and buckling or fracture of the frame members or connections. The required amount of energy dissipation to limit drift is discussed first, followed by discussion of the three strength-degrading limit states.

If the fuse strength is too small relative to the PT force, the reduced amount of energy dissipation may lead to unacceptably large earthquake drifts. As shown in Fig. 11, the energy dissipation of a self-centering hysteretic behavior can be expressed as a ratio normalized to the energy dissipation of a bilinear (elastic linear hardening) system. Figs. 11(b and c) graphically show energy dissipation ratios of 50 and 25% respectively. Based on these idealized hysteresis loop shapes, the energy dissipation ratio, ED, is calculated according to Eq. (12) as the ratio of M_{flag} [Eq. (6)] to $2M_y$ [Eq. (1)]. When the PT stiffness and fuse-hardening stiffness are assumed to be equal, the ED ratio simplifies to the ratio of fuse to total overturning resistance. The degrading fuse factor, α_d, is unity for nondegrading fuses, as is shown in Fig. 7(c), and would be the ratio of the degraded fuse hysteretic energy to the hysteretic energy of an idealized elastic linear hardening fuse

$$\mathrm{ED} \cong \alpha_d \frac{M_{\mathrm{flag}}}{2M_y} \cong \alpha_d \frac{M_{\mathrm{fsy}}}{M_y} \tag{12}$$

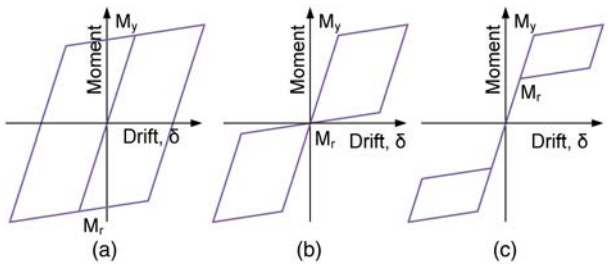

Fig. 11. Variation in energy dissipation capability: (a) 100% energy dissipation; (b) 50% energy dissipation; (c) 25% energy dissipation

Some guidance for the lower limit on energy dissipation ratio is available in the literature. Christopoulos et al. (2002) found that the minimum energy dissipation ratio required to produce similar ductility demands between elastic perfectly plastic systems and inelastic flag-shaped hysteretic systems depends on the post-yield stiffness of the flag-shaped systems. Seo and Sause (2005) further found that for a post-yield stiffness equal to 20 and 10% of the initial stiffness, energy dissipation ratios of 12.5 and 25%, respectively, produced similar ductility demands as conventional systems. Eatherton and Hajjar (2010) found that the peak drifts of self-centering systems became less sensitive to the energy dissipation ratio when the energy dissipation ratio was above 25%. The ACI ITG (2009) provisions for rocking precast concrete walls require a minimum energy dissipation ratio of 12.5% between the nonlinear rocking system and an equivalent elastically perfectly plastic system. This ratio of 12.5% is roughly equivalent to the ratio of 25%, as normalized to the elastic–linear hardening system of Fig. 11(a). The relationship between these two energy measures is not constant and depends on the nonlinear response, but the ratio of two was found to be representative of the cyclic response of rocking steel frames at reasonably large drifts—on the order of 2% drift (Eatherton and Hajjar 2010). Unless the analysis to determine the drift demand explicitly considers variable hysteretic energy dissipation (damping), it is suggested to maintain an ED ratio larger than 25%. For the simplified case, where the PT and fuse-hardening ratios are assumed equal, the minimum ED ratio of 25% [Eq. (12)] corresponds to a maximum SC ratio [Eq. (9)] of 3.0 for a nondegrading fuse.

PT Yield and Fracture

The PT should be proportioned to prevent yield under the expected frame uplift for DBE demands and to prevent fracture under MCE demands. Several design parameters contribute to the change in PT force and strain demands under increasing drift [Eqs. (2), (4), and (5)], including the location of the PT relative to the pivot point, X_{PT}, the initial PT stress, $F_{\mathrm{pti}}/A_{\mathrm{PT}}$, and length of PT, L_{PT}. Assuming rigid body rotation of the frames, the criteria for allowing enough PT deformation capacity so that the frames can reach a target drift ratio, $(\delta/H)_{\mathrm{target}}$, is given in Eq. (13) where $\varepsilon_{\mathrm{limit}}$ is the limiting strain for the PT

$$\varepsilon_{\mathrm{peak}} = \frac{F_{\mathrm{pti}}}{A_{\mathrm{PT}}E_{\mathrm{PT}}} + \frac{X_{\mathrm{PT}}(\delta/H)_{\mathrm{target}}}{L_{\mathrm{PT}}} \leq \varepsilon_{\mathrm{limit}} \tag{13}$$

Stress and strain limits on PT depend, first, on the type of PT (high strength bar versus strand systems) and, second, on the PT material and the anchorage system. Experiments on the rocking frames with strands showed that when PT strands are elongated past the elastic limit, there is a potential to fracture individual wires in the multiwire strands. Typically, the individual wire fractures do not precipitate sudden fractures in other wires or strands and thus do not result in sudden strength loss. Nonetheless, fractures should be avoided at least up to MCE drift demands. For high strength strands with ultimate strengths of 1,860 MPa (270 ksi), the available evidence suggests that strands may begin to fracture at strains exceeding about 1% (Eatherton and Hajjar 2010), although it should be emphasized that the fracture strain is dependent on the specific strand and anchorage system (e.g., as evident in tests reported by Walsh and Kurama 2012 and Ma et al. 2011). Based on available data, it is recommended to limit the maximum PT strand strains, $\varepsilon_{\mathrm{peak}}$, to 1% for roof drift ratios, δ/H, under MCE ground motion intensities and 0.8% for the DBE hazard level. The 1% strain limit is also recommended by ACI ITG (2009) for PT precast

walls. post-tensioning bars have been shown to undergo more yielding prior to fracture, thus a larger strain limit for PT bars may be appropriate.

Fuse Fracture

Fracture of the energy-dissipating fuses could likewise lead to significant strength degradation. It is therefore necessary to limit the probability of fuse fracture at the displacements associated with the MCE. Tested butterfly fuse panels underwent increasing cyclic deformations up to effective shear strains of 30 to 45%, measured across the link length (Dimension L in Fig. 7), before experiencing fracture (Ma et al. 2010). Alternatively, deformation capacities of buckling restrained brace (BRB) fuses, can be obtained from BRB standards and manufacturer tests. The deformation capacities of the butterfly or BRB fuses can be related to deformation demands, which depend on the rocking frame system configuration and earthquake ground motion intensity. Further details of procedures for assessing fuse fracture limit states are included in Eatherton and Hajjar (2010) and Ma et al. (2010, 2011).

Rocking Frame Integrity

Another potential strength-degrading limit state is significant yielding, buckling, or fracture in the braced frame or its connections. The rigid body frame rotation correlates with and effectively reduces the base shear related to the first mode response as compared to an elastic braced frame. However, lateral seismic forces associated with higher modes are not reduced much because the base rocking has little, if any, contribution to the higher mode shapes (e.g., Fig. 6). Thus, where higher modes are significant, the story shears in the rocking frames can be much larger than those predicted based on the first-mode dominant equivalent lateral forces associated with the base moment, $M(\delta/H)$, given by Eqs. (5) and (8). This phenomenon is not unique to the rocking steel frames and is observed in other spine-type lateral force-resisting systems, such as concrete shear walls. Three alternative proposed methods for calculating peak story shears and the resulting member forces for design of the rocking frame include ones that either (1) modify forces calculated by linear static analysis (Eatherton and Hajjar 2010; Ma et al. 2011), (2) modify forces calculated by linear dynamic or response spectrum analysis (Roke et al. 2009), or (3) calculate the forces directly by nonlinear time history analyses.

Aside from the member forces resulting from the induced story shears, column compression pulses induced by impact of the rocking frame column bases is a commonly raised question related to the frame integrity. In rocking bridge piers analyzed by Pollino and Bruneau (2004), column impact was found to be a significant effect, since the bridge weight exerts both vertical and lateral inertial effects on the rocking columns. However, in the building systems, this effect is much less significant, since the tributary vertical mass on the rocking columns is typically quite small (e.g., Fig. 4) relative to the tributary seismic mass that is stabilized by the rocking frame. Moreover, unlike free-rocking cases often examined in the literature, the rocking response of the proposed systems is controlled by the presence of yielding fuses. As a result, the forces that develop upon impact of the uplifted columns are usually much smaller than the governing compression load condition for the pivoting columns, which occurs when the frame is at its peak rocking rotation and the columns in contact with the ground are resisting compression forces developed by the full gravity load on the frame and the downward acting forces applied to the frame by the PT and yielded fuse. This behavior has been borne out by tests and analyses by Eatherton et al. 2014) and Ma et al (2011).

Seismic Design and Proportioning of System Components

Once the overall configuration of the rocking frame system is established, the first step in design is to establish the minimum required overturning resistance [Eq. (7)], which can be related to the minimum required base shear based on an assumed lateral force distribution [Eq. (8)]. As a starting point, it is suggested to do this using the ASCE 7 (2010) base shear and equivalent lateral force procedure, with an R value of 8 (equivalent to other ductile systems). The required design strength [Eqs. (1) and 7)] can then be used to establish minimum requirements for the strength provided by the combined contributions of PT, tributary dead load, and the energy dissipating fuse. The self-centering [Eqs. (9) and (10)], global uplift [Eq. (11)] and minimum energy dissipation [Eq. (12)] can then be used to help establish an appropriate balance between the fuse shear strength, V_{fp}, and the initial PT force, F_{pti}. As indicated previously, limits on these contributions are controlled by maintaining SC and UL ratios [Eqs. (9) and (11)] larger than 1.0 and an ED ratio [Eq. (12)] larger than 0.25 to help ensure good performance.

Once the required initial PT force is determined, then the initial PT stress and resulting PT area can be calculated. Typically, the most economical design is achieved by setting the initial PT stress as high as possible and the area of PT as small as possible, while checking that the maximum strains are limited to prevent fracture under MCE drift demands [Eq. (13)]. As noted previously, a limit of 1% strain is suggested for the fracture limit state of Grade 270 PT strand systems. Aside from minimizing the cost of the PT itself, minimizing the PT cross-sectional area minimizes the post-uplift hardening [Eq. (4)], the associated base moments [Eq. (5)] and related forces that develop under rocking. Thus, the smaller PT area will reduce the additional force the PT imposes on the braced frame, and thus can result in more economical frame design. The reduced post-uplift stiffness [Eq. (4)] will, however, tend to increase the post-uplift displacements, which can be examined by calculating the drift ratio at fuse yield. Thus, there are competing factors to consider in deciding upon the appropriate initial PT stress and cross-sectional area.

The choice of whether to use PT strands or bars can also affect which limit states control the design. post-tensioning strands have larger elastic strain capacity but little post-yield deformation capacity before wire fracture. In Fig. 10, this would be represented by PT yield (3) and strength degradation (5) being close together resulting in strength degradation as the likely controlling limit state. Conversely, PT bars allow significant yielding before fracture, thus causing PT yield (3) well before strength degradation (5). In this case, global uplift and loss of self-centering are more likely to be the controlling limit states.

The choice of fuse type (degrading versus nondegrading) as well as fuse location have important effects on system behavior. As inferred from Eqs. (9) and (11), significant hardening in the fuse can make it more difficult to retain self-centering ability and prevent global uplift. Degrading fuses, on the other hand, will enhance self-centering, but the reduced energy dissipation to values below the suggested minimum of ED equal to 0.25 may result in larger drifts.

The PT and fuse requirements will obviously depend on the system configuration (Fig. 3), building height (Fig. 6), and the geometry (Fig. 9). Locating the PT and/or fuses at the center of the frame results in half the displacement demands as compared to components located at the column lines. Fuses up the height of the frame, which can be accommodated in the dual-frame configuration or in the single-frame configuration with multiple hinge

(rocking) points (Figs. 3 and 6), will dissipate energy of higher modes, although self-centering of higher mode deformations may be affected in the dual configuration because the PT restoring force only acts to close the base gap.

Once the PT and fuse components are designed, the overall system can be designed considering the expected drifts and imposed braced frame member forces under DBE and MCE ground motions. In the event that the drifts are larger than desired or other limits are not met, the PT and fuse components can be adjusted to modify the system yield strength, M_y, and/or its hardening stiffness, K_{up} and K_3. Further details of proposed methods for calculating drifts and internal member forces are discussed elsewhere (Eatherton and Hajjar 2010; Ma et al. 2011) and remain a topic of ongoing study.

Example Applications

The design concepts and equations presented previously are demonstrated by application to a six-story prototype building with the floor plan of Fig. 4. Designs for a 9.14-m (30-ft) wide single-frame configuration and dual-frame configuration with 3.81-m (12.5-ft) wide frames and 1.52-m (5-ft) centerline column spacing between frames were developed. The lateral design forces are calculated using the equivalent lateral force method in ASCE 7 (ASCE 2010) using the approximate formula given therein for steel-braced frames to calculate the fundamental period. This is justified by analysis and measurements comparing the initial stiffness of rocking steel frames to concentrically braced steel frames (e.g., Eatherton and Hajjar 2010). Based on a high seismic region and response modification factor, $R = 8$, the required design base shear ratio was computed to be $V/W = 0.125$, and the required moment strength is given in Table 1. An SC ratio of 1.9 is used for the single-frame configuration and 1.25 for the dual-frame configuration. A higher SC ratio was used for the single-frame configuration as a precaution to ensure that the global uplift requirement is met, even in the event of modest PT losses and fuse hardening as verified at the bottom of Table 1. The moment arm for the fuse in the dual-frame configuration is larger than the moment arm for the PT, allowing smaller SC ratio while providing similar resistance to global uplift.

Table 1. Summary of Design Information

Quantity	Single frame	Dual frame
Required strength		
Base shear ratio, V_u/W	0.125	0.125
Overturning moment, M_u (kN-m)	30,941	30,941
Geometric parameters		
Fuse eccentricity, X_{fs} (m)	2.11	4.78
PT eccentricity, X_{PT} (m)	5.54	4.78
Dead load eccentricity, X_D (m)	4.01	9.35
System proportioning		
Self-centering ratio, SC	1.25	1.90
Initial PT force, F_{pti} (kN)	3,452	2,500
Fuse shear strength, V_{fp} (kN)	2,758	2,482
Uplift ratio, UL	1.66	1.46
Component strength and details		
Number of PT strands per frame	20	24
PT area, A_{PT} (mm^2)	2,800	3,360
Initial PT stress (F_{pti}/F_{ptu})	0.66	0.40
Expected dead load, P_{De} (kN)	1,133	1,133
Expected system behavior		
Moment capacity, M_n (kN-m)	34,372	34,380
Stiffness, K_{up} (kN-m/rad)	205,715	633,251
Flag height, M_{flag} (kN-m)	30,542	23,705
Energy dissipation ratio, ED	0.44	0.34
Behavior after displacement to 3% drift ratio		
Peak moment, M_{MCE} (at 3% Drift)	42,405	53,150
Peak PT strain, ε_{peak} (%)	0.89%	0.98%
After yielding, F^*_{pti} (kN)	3,452	1,929
Hardened fuse force, V^*_{fp} (kN)	3,370	3,078
SC ratio after drift to 3%, SC*	1.02	1.35
UL ratio after drift to 3%, UL*	1.36	0.99

The equations for minimum strength [Eq. (7)] and SC ratio [Eq. (9)] were then solved simultaneously to determine the required fuse shear strengths and initial PT forces given in Table 1. A resistance factor, $\phi = 0.9$ was used in Eq. (7) similar to common values for flexural yielding since the fuse shear capacity is governed by flexural yielding of the links, recognizing that further investigation may be warranted to determine the level of variability in the uplifting moment. The number of 15-mm diameter PT strands was determined to limit the peak PT strain as calculated using Eq. (13) to 1.0% when the frames are subjected to 3.0% rigid body rotation. A limiting roof drift ratio of 3% is used for the MCE level demand, which is conservatively chosen as 1.5 times the default drift limit of 2% for DBE demands in ASCE 7. The 3% limit also corresponds to the value recommended for the performance-based design of tall buildings (e.g., PEER 2010). Moreover, studies of nonlinear response history analyses of 23 prototype rocking frames reported median roof drift ratios between 1.7 to 3.3% with an average value of 2.4%, indicating that the 3% drift limit is reasonable (Eatherton and Hajjar 2010; Ma et al. 2011). The study by Ma et al. (2011) recommends a practical method to calculate the inelastic (post-uplift) drift demand based on spectral acceleration demands and an effective period, which is determined using a secant stiffness obtained from the idealized system rocking response [e.g., Fig. 8(b) or 10] at the target displacement. The resulting PT areas and initial PT stress ratios are given in Table 1. The fuses could be designed using equations provided in Ma et al. (2010) for the strength given in Table 1. Similarly, the frame members could be designed using an amplified linear static analysis method described in Eatherton and Hajjar (2010).

The fuse stiffness, K_{fs}, was assumed to produce fuse yield at 0.5% drift, whereas frame stiffness, K_{fr}, and fuse-hardening ratio were assumed to be three times the fuse stiffness and 3% of the initial fuse stiffness respectively. The post-yield stiffness, K_{up}, hysteretic flag height, M_{flag}, and energy dissipation ratio, ED, were calculated using Eqs. (4), (6), and (12), respectively. The energy-dissipation ratio is shown satisfactory in that it is greater than 0.25.

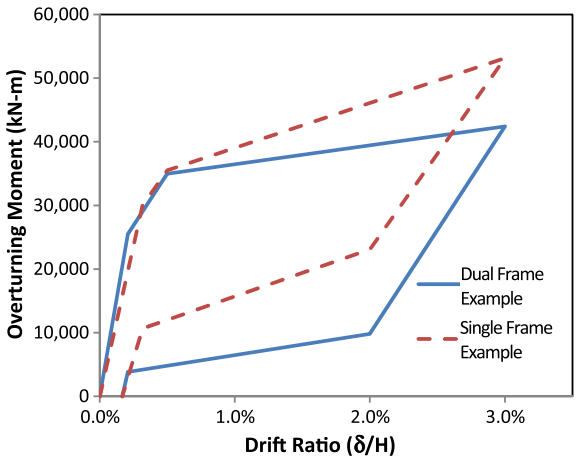

Fig. 12. Idealized drift versus overturning moment for rocking frame examples

The behavior of the system as it is subjected to a drift ratio of 3% is examined using the equations presented above. The peak strains and associated force loss in the post-tensioning were computed using Eqs. (10) and (13), assuming a post-tensioning yield stress of 1,758 MPa (255 ksi) and neglecting seating losses. Based on the reduced post-tensioning force and hardened-fuse force, the self-centering ratio and uplift ratio were computed and are given in Table 1. The dual-frame configuration self-centering ratio is shown to drop from 1.25 to 1.02 after cycles up to 3.0% drift. On the other hand, the single-frame uplift ratio is shown to drop from 1.46 to 0.99. Since both are close to the target of 1.0, they may be considered acceptable to produce self-centering while resisting global uplift, but these examples demonstrate the importance of examining the system behavior after PT losses and fuse hardening to produce desirable performance after large drift cycles. The resulting idealized cyclic pushover curves for the two designs are shown in Fig. 12, where one can see that the base overturning moment demands at the expected MCE drift of 3% is 21 and 50% larger than the yield moment, M_y, for the dual-frame and single-frame configurations respectively. The importance of the uplifting stiffness, K_{up}, is demonstrated as it has a significant effect on system overstrength.

Conclusions

The steel self-centering rocking frame system is capable of providing enhanced seismic performance by virtually eliminating residual drifts and concentrating structural damage in replaceable fuse elements. While different configurations of the system are possible, the main characteristics of the system include a stiff braced frame spine that helps enforce uniform story drifts and is allowed to uplift and rock at its base, vertical PT that resists overturning and provides an elastic restoring force to close the uplifting gap, and replaceable structural fuses that resist overturning and dissipate energy and thereby damp earthquake-induced motions. When properly proportioned, the post-tensioned frame and energy-dissipating fuses result in a flag-shaped hysteresis force–deformation curve that is characteristic of self-centering systems.

Equations to describe the overall base moment versus uplift rotation were presented, along with discussion and guidance for key design limit states. The suggested strength criteria for the initial limit states of column uplift and fuse yielding are intended to be commensurate with yield strength limits for other ductile seismic systems. Limit states that should be prevented under DBE ground motions mostly relate to yielding and losses in PT that can degrade the self-centering response. Limit states that should be prevented under MCE ground motions are those that can lead to significant degradation of system strength, such as global uplift, fracture of the fuse elements or PT, or significant yielding and potential failures in the braced frame members and connections. These methods for proportioning the PT and fuse in a single-frame configuration and dual-frame configuration system were illustrated through a design example and the ability of these types of rocking frames to successfully control the progression of limit states is shown through computational analyses presented in the literature (Eatherton and Hajjar 2010; Ma et al. 2011).

The design concepts and equations presented in this paper are intended to outline some of the main aspects of the rocking frame design. Due to space and other limitations, there are several important aspects of the design and behavior that are not addressed here, including calculation of earthquake-induced drifts and member forces. These and other aspects of the design can be integrated into the proposed framework. Finally, in addition to establishing a basis for design, the proposed framework provides the basis to interpret experimental and analytical studies to validate certain aspects of design and behavior, two of which are reported in companion studies by Eatherton et al. (2014) and Ma et al. (2011).

Acknowledgments

The authors greatly appreciate the contributions to this work from graduate students Kerry Hall, Eric Borchers, and Alex Peña, postdoctoral researcher Paul Cordova, and practicing structural engineer Gregory Luth. The authors also thank our Japanese collaborators, professors Toru Takeuchi, Mitsumasa Midorikawa, Masayoshi Nakashima, Kazuhiko Kasai, researcher at E-Defense Tsuyoshi Hikino, and graduate students Ryota Matsui, Masaru Oobayashi, Yosuke Yamamoto, and Ryohei Yamazaki. This material is based upon work supported by the National Science Foundation under Grant No. (CMMI-0530756) via the George E. Brown, Jr. Network for Earthquake Engineering Simulation, the American Institute of Steel Construction, Stanford University, and the University of Illinois at Urbana-Champaign.

References

ACI ITG. (2009). "Requirements for design of special unbonded post-tensioned precast shear wall satisfying ACI ITG-5.1 (ACI ITG-5.2-09) and commentary." *ACI ITG -5.2-09*, Reported by ACI Innovation Task Group 5, Farmington Hills, MI.

Ajrab, J. J., Pekcan, G., and Mander, J. B. (2004). "Rocking wall-frame structures with supplemental tendon systems." *J. Struct. Eng.*, 10.1061/(ASCE)0733-9445(2004)130:6(895), 895–903.

ASCE/SEI 7-10. (2010). *Minimum design loads for buildings and other structures*, Structural Engineering Institute, Reston, VA.

ATC. (1995). *ATC-20-2 Addendum to the ATC-20 postearthquake building safety evaluation procedures*, Redwood City, CA.

ATC. (2012). *FEMA P-58 seismic performance assessment of buildings*, Redwood City, CA.

Azuhata, T., Ishihara, T., Midorikawa, M., and Wada, A. (2006). "Seismic response of steel frames with multi-spans by applying rocking structural system." *Proc., 5th Int. Conf. on Behaviour of Steel Structures in Seismic Areas STESSA 2006*, Taylor & Francis Group, London, U.K.

Bazzurro, P., Cornell, C. A., Menun, C., and Motahari, M. (2004). "Guidelines for seismic assessment of damaged buildings." *Proc., 13th World Conf. on Earthquake Engineering*, Mira Digital Publishing, Vancouver, BC, Canada.

Chen, Y.-H., Liao, W.-H., Lee, C.-L., and Wang, Y.-P. (2006). "Seismic isolation of viaduct piers by means of a rocking mechanism." *Earthquake Eng. Struct. Dynam.*, 35(6), 713–736.

Christopoulos, C., Filiatrault, A., and Folz, B. (2002). "Seismic response of self-centering hysteretic SDOF systems." *Earthquake Eng. Struct. Dynam.*, 31(5), 1131–1150.

Clough, R. W., and Huckelbridge, A. A. (1977). "Preliminary experimental study of seismic uplift of a steel frame." *Rep. No. UCB/EERC-77-22*, Earthquake Engineering Research Center (EERC), Univ. of California, Berkeley, CA.

Eatherton, M. R., and Hajjar, J. F. (2010). "Large-Scale cyclic and hybrid simulation testing and development of a controlled-rocking steel building system with replaceable fuses." *Rep. No. NSEL-025*, Newmark Structural Engineering Laboratory Report Series, Univ. of Illinois at Urbana-Champaign, Urbana, IL.

Eatherton, M. R., and Hajjar, J. F. (2011). "Residual drifts of self-centering systems including effects of ambient building resistance." *Earthquake Spectra*, 27(3), 719–744.

Eatherton, M. R., Ma, X., Krawinkler, H., Deierlein, G. G., and Hajjar, J. F. (2014). "Quasi-static cyclic behavior of controlled rocking steel frames." *J. Struct. Eng.*, 10.1061/(ASCE)ST.1943-541X.0001005, 04014083.

Fahnestock, L. A., Ricles, J. M., and Sause, R. (2007). "Seismic response and performance of buckling-restrained braced frames." *J. Struct. Eng.*, 10.1061/(ASCE)0733-9445(2007)133:9(1195), 1195–1204.

FEMA. (2009). *Quantification of building seismic performance factors FEMA P695*, Federal Emergency Management Agency.

Gledhill, S. M., Sidwell, G. K., and Bell, D. K. (2008). "The damage avoidance design of tall steel frame buildings—Fairlie terrace student accommodation project, Victoria University of Wellington." *New Zealand Society for Earthquake Engineering 2008 Conf.*, New Zealand Society for Earthquake Engineering, Wellington, New Zealand.

GPLA. (2012). "Personal correspondence with Gregory P. Luth on Isle of Capri Casino in Cape Girardeau, MO." ⟨http://www.gregorypluth.com⟩ (May 22, 2012).

Hall, K. S., Eatherton, M., and Hajjar, J. F. (2010). "Nonlinear behavior of controlled rocking steel-framed building systems with replaceable energy dissipating fuses." *Rep. No. NSEL-026*, Newmark Structural Engineering Laboratory Report Series, Urbana, IL.

Housner, G. W. (1963). "The behavior of inverted pendulum structures during earthquake." *Bull. Seismological Society of America*, 53(2), 403–417.

Iwata, Y., Sugimoto, H., and Kuwamura, H. (2006). "Reparability limit of steel buildings based on the actual data of the Hyogoken-Nanbu earthquake." *Wind and Seismic Effects Proc., 38th Joint Panel Meeting*, NIST Special Publication 1057, NIST, Gaithersburg, MD.

Lai, J.-W., Chen, C.-H., and Mahin, S. A. (2010). "Experimental and analytical performance of concentrically braced steel frames." *Proc., 2010 Structures Congress*, ASCE, Reston, VA.

Lu, Y. (2005). "Inelastic behaviour of RC wall-frame with a rocking wall and its analysis incorporating 3-D effect." *Struct. Design Tall Specl. Build.*, 14(1), 15–35.

Luco, N., Bazzuro, P., and Cornell, C. A. (2004). "Dynamic versus static computation of the residual capacity of a mainshock-damaged building to withstand an aftershock." *Proc., 13th World Conf. on Earthquake Engineering*, Mira Digital Publishing, St. Louis, MO.

Ma, X., Borchers, E., Peña, A., Krawinkler, H., and Deierlein, G. (2010). *Design and behavior of steel shear plates with openings as energy-dissipating fuses*, Blume Earthquake Engineering Center, TR 173, Stanford Univ., Stanford, CA.

Ma, X., Krawinkler, H., and Deierlein, G. G. (2011). "Seismic design and behavior of self-centering braced frame with controlled rocking and energy dissipating fuses." *Rep. No. 174*, The John A. Blume Earthquake Engineering Center, Stanford Univ., Stanford, CA.

Mander, J. B., and Cheng, C. T. (1997). *Seismic resistance of bridge piers based on damage avoidance design*, *Technical Rep. No. NCEER-97-0014*, Univ. of Buffalo, Buffalo, NY.

Mar, D. (2010). "Design examples using mode shaping spines for frame and wall buildings." *9th US National and 10th Canadian Conf. on Earthquake Engineering*, Mira Digital Publishing, St. Louis, MO.

McCormick, J., Aburano, H., Ikenaga, M., and Nakashima, M. (2008). "Permissible residual deformation levels for building structures considering both safety and human elements." *Proc., 14th World Conf. on Earthquake Engineering*, Mira Digital Publishing, St. Louis, MO.

PEER. (2010). "Guidelines for performance-based seismic design of tall buildings." *Rep. 2010/05*, prepared by the TBI Guidelines Working Group, Pacific Earthquake Engineering Research Center, Univ. of California, Berkeley, CA.

Pollino, M., and Bruneau, M. (2004). "Seismic retrofit of bridge steel truss piers using a controlled rocking approach." *Technical Rep. MCEER-04-0011*, Univ. of Buffalo, Buffalo, NY.

Priestley, M. J. N., Sritharan, S., Conley, J. R., and Pampanin, S. (1999). "Preliminary results and conclusions from the PRESS five-story precast concrete test building." *PCI J.*, 44(6), 42–54.

Ramirez, M., and Miranda, E. (2012). "Significance of residual drifts in building earthquake loss estimation." *Earthquake Eng. Struct. Dynam.*, 41(11), 1477–1493.

Roke, D., Sause, R., Ricles, J. M., and Gonner, N. (2009). "Damage-free seismic-resistant self-centering steel concentrically-braced frames." *Proc., 6th Int. Conf. on Behaviour of Steel Structures in Seismic Areas (STESSA)*, Taylor & Francis Group, London, U.K.

Sause, R., Ricles, J. M., Roke, D. A., Chancellor, N. B., and Gonner, N. P. (2010). "Seismic performance of a self-centering-rocking concentrically-braced frame." *Proc., 9th U.S. National and 10th Canadian Conf. on Earthquake Engineering*, Mira Digital Publishing, St. Louis, MO.

Seo, C.-Y., and Sause, R. (2005). "Ductility demands on self-centering systems under earthquake loading." *ACI Struct. J.*, 102(2), 275–285.

Tipping-Mar. (2012). "Packard foundation headquarter building." Los Altos, CA, ⟨http://www.tippingmar.com/projects/project_details/43⟩ (May 22, 2012).

Tremblay, R., et al. (2008). "Innovative viscously damped rocking braced steel frames." *14th World Conf. on Earthquake Engineering*, Beijing, China.

Wada, A., Yamada, S., Fukuta, O., and Tanigawa, M. (2001). "Passive controlled slender structures having special devises at column connections." *7th Int. Seminar on Seismic Isolation, Passive Energy Dissipation and Active Control of Vibrations of Structures*, European Association of Earthquake Engineering, Istanbul, Turkey.

Walsh, K. Q., and Kurama, Y. C. (2012). "Effects of loading conditions on the behavior of unbondend post-tensioning strand-anchorage systems." *PCI J.*, 57(1), 76–96.

Wiebe, L., and Christopoulos, C. (2009). "Mitigation of higher mode effects in base-rocking systems by using multiple rocking sections." *J. Earthquake Eng.*, 13(S1), 83–108.